Pertanika J. Sci. & Technol. 32 (2): 741 - 760 (2024)

PERTANIKA JOURNALS

SCIENCE & TECHNOLOGY

Journal homepage: http://www.pertanika.upm.edu.my/

Microencapsulation of *Acalypha indica* Linn. Extracts Using Chitosan-Polycaprolactone Blends

Maizatul Akmal Johari[1], Fathilah Ali[1]*, Azlin Suhaida Azmi[1], Hazleen Anuar[2], Jamarosliza Jamaluddin[3] and Rosnani Hasham[4]

[1]Department of Chemical Engineering and Sustainability, Kulliyyah of Engineering, International Islamic University Malaysia, 50728 Kuala Lumpur, Malaysia
[2]Department of Manufacturing and Materials Engineering, Kulliyyah of Engineering International Islamic University Malaysia, 50728, Kuala Lumpur, Malaysia
[3]Department of Chemical Engineering, Faculty of Chemical and Energy Engineering, Universiti Teknologi Malaysia, 81310 Johor Bahru, Johor, Malaysia
[4]Department of Bioprocess and Polymer Engineering, Faculty of Chemical and Energy Engineering, Faculty of Engineering, Universiti Teknologi Malaysia, 81310 Johor Bahru, Johor, Malaysia

ABSTRACT

Polymer encapsulation is commonly adopted in drug delivery systems to form encapsulation that can assist in delivering active compounds to the targeted area. *Acalypha indica* (AI) crude extract was obtained from AI plants through ultrasound-assisted extraction. It is naturally unstable in the external environment and, thus, needs to be encapsulated to protect against volatility. Herein, this study emphasized the development of the encapsulations of AI extracts using a chitosan-polycaprolactone (PCL) blend by emulsion-solvent evaporation and freeze-dried methods. Four parameters for Al encapsulation were studied by fixing one parameter at a time. The percentage of encapsulation efficiency (EE%) was recorded as a response for each parameter. The study proceeded with central composite design (CCD) as the response surface methodology (RSM) optimization tool to study the interactions between the factors. Central points were taken from the preliminary data obtained in one-parameter experiments. The validation was carried out with two data of the highest and lowest EE% suggested by CCD. The highest EE% recorded was 98.70%, and the lowest EE% was 87.80%. The results showed a difference between predicted and experimental values at a percentage lower than 7.5%. Fourier Transform Infrared Spectroscopy (FTIR),

ARTICLE INFO

Article history:
Received: 28 January 2023
Accepted: 17 August 2023
Published: 14 March 2024

DOI: https://doi.org/10.47836/pjst.32.2.14

E-mail addresses:
maiez.akmal93@gmail.com (Maizatul Akmal Johari)
fathilah@iium.edu.my (Fathilah Ali)
azlinsu76@iium.edu.my (Azlin Suhaida Azmi)
hazleen@iium.edu.my (Hazleen Anuar)
jamarosliza@utm.my (Jamarosliza Jamaluddin)
r-rosnani@utm.my (Rosnani Hasham)
* Corresponding author

ISSN: 0128-7680
e-ISSN: 2231-8526

scanning electron microscopy (SEM), particle size analyzer, and zeta potential were used to analyze the properties of selected microencapsulated samples. Overall, the encapsulation of AI extracts was successful and has the potential to be used in drug delivery.

Keywords: Acalypha indica Linn., central composite design, chitosan, microencapsulation, polycaprolactone

INTRODUCTION

Over the past decades, a lot of research and invention has been done and keeps growing to enhance the current drug delivery system (Yusuf et al., 2023). In developing a good controlled-release drug delivery system, selecting a good drug carrier is the most challenging in the sense that the side effects of the drugs and the drug carriers on humans can be minimized (Adepu & Ramakrishna, 2021). Chitosan has been proven to be an effective polymeric drug carrier. Chitosan is found naturally from aquatic shell wastes and is one of the most abundant polymers in nature, thus providing a vast potential for commercial value. Due to good mucoadhesive properties and biodegradability, chitosan is safe for consumption (Roy & Sahoo, 2016; Szymańska & Winnicka, 2015). However, chitosan needs modification to improve its stability and solubility to form an excellent polymer matrix for microencapsulation. The limitations of chitosan can be improved through several methods of modification while maintaining the parent chain. In this way, the modification preserves the good physicochemical properties. Physically blending with another polymer is one of many ways to improve the characteristics of chitosan.

Recently, encapsulation studies have focused more on synthetic pharmaceutical drugs. However, encapsulations of certain plant extracts are somehow less explored. The challenges of maintaining stable *Acalypha indica* (AI) extracts are related to the fact that the active compounds are naturally volatile, light and temperature sensitive and susceptible to degradation (Bazana et al., 2019). AI, commonly known as Indian copperleaf, is an herbaceous species plant. However, it gets less attention because its habitat is mostly in the backyards and is often treated as a weed. However, AI can be found only in certain geographical regions (El Hady et al., 2019). Interestingly, there is a fascinating fact about this plant and its high potential for commercialization.

Previously, it was reported that the leaf extracts of AI have several bioactive compounds that can treat respiratory problems such as bronchitis, asthma, and pneumonia (Martin & Ashokkumar, 2017; Taurozzi et al., 2012). Poly-ε-caprolactone (PCL) is a biodegradable aliphatic polyester with better viscoelastic and allows many structures such as microspheres. Due to its properties, PCL can be easily blended with other polymers, such as chitosan, for microencapsulations (Christen & Vercesi, 2020).

Modifying the chitosan with PCL via blending can benefit the immobilization of the AI extracts against any interactions with the external environment through encapsulation (Rivas

et al., 2019). Encapsulation is very vital as without encapsulation, and the uncontrolled environmental condition has a tendency to break down certain types of beneficial bioactive compounds of the AI extracts.

The emulsion-solvent evaporation method is identified as the most suitable method to encapsulate the ethanolic AI extracts. The microencapsulation of AI extracts was conducted by blending chitosan with a PCL. First, experiments were done by fixing one factor at a time (OFAT) for four parameters: homogenization duration, the ratio of chitosan: PCL, the concentration of surfactant (PVA), and polymer matrix concentrations. Subsequently, an optimization study of the three factors (ratio of chitosan: PCL concentration, PVA concentration, and Concentration of chitosan-PCL blend) was performed using the design of experiments (DOE) by central composite design (CCD), and the percentage of encapsulation efficiency (EE%) was recorded as the response. Lastly, the microcapsules were characterized with SEM, FTIR, zeta potential and particle size analysis.

MATERIALS AND METHODS

Materials and Instrumentations

Chitosan (medium molecular weight 190,000-310,000 Da, Catalog No. 448877, ~85% deacetylated), poly-(ε-caprolactone)(PCL) (molecular weight= 45,000 Da, SKU No. 704105), and poly(vinyl alcohol) (PVA) (molecular weight= 31,000–50,000 Da, SKU No. 363138, 98%–99% hydrolyzed), were purchased from Sigma Aldrich, USA. Methylene chloride (DCM) (Catalog No. 106050, 84.93 g/mol) was purchased from Merck Millipore®, Germany. Acetic acid glacial (60.05 g/mol) analytical grade was purchased from Bendosen Laboratory Chemicals, Norway. *Acalypha indica* (AI) extracts were obtained from Universiti Teknologi Malaysia (UTM) through ultrasound-assisted extraction using a water bath sonicator and ethanol as the solvent. Anhydrous ethanol, 99.8% v/v absolute denatured grade, was purchased from HmbG® Chemicals, Germany.

Fabrication of Chitosan-PCL Encapsulation-loaded *Acalypha indica* Extract

Following the previously reported method, the physical blending of the chitosan-PCL was done according to the emulsion-solvent evaporation method (El Hady et al., 2019). The mechanism of AI extract encapsulation was simplified, as shown in Figure 1.

Firstly, a fixed parameter was conducted per the aforementioned method following the recipe in Table 1. PCL (0.5%) was dissolved in an organic phase of DCM, PVA (2%) in deionized water, and chitosan (0.5%) in 0.2%v/v aqueous acetic acid. Then, the polymer solutions were vigorously stirred for 24 hours to dissolve the polymers, and PVA was stirred at a temperature of 60 °C. The AI extract was diluted in ethanol to get a concentration of 0.2 g/mL.

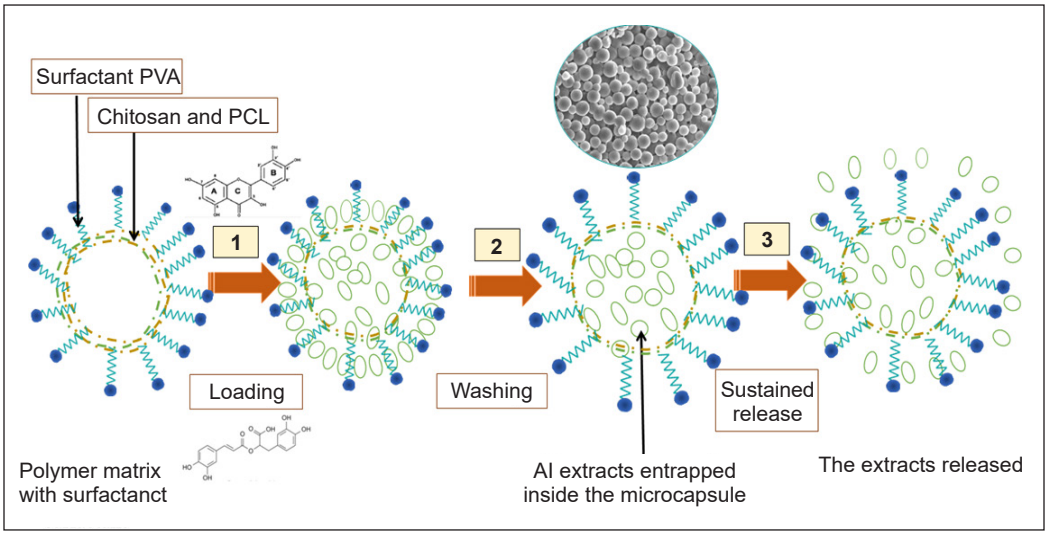

Figure 1. The overview process of encapsulation of AI extracts and the extract release

Next, the microencapsulation of *Acalypha indica* (AI) extract was fabricated. A 5 mL emulsion of PCL was transferred into a 50 mL-sized tube containing 5 mL of PVA. Then, 5 mL of each PCL, chitosan, and the AI extract were sequentially added. Immediately, solutions were homogenized under an ultrasonic homogenizer (Fisher Scientific FB705,700 watts) with an amplitude of 90% and homogenized to form a water-in-oil (W/O) emulsion. After that, the solutions were moderately stirred with a magnetic stirrer for 24 hours at room temperature in a controlled environment. After that, the microparticles were collected by centrifuging at 13,000 rpm for 1 hour using a mini centrifuge (Eppendorf, speed x 1,000). Two layers of supernatant and precipitates were formed. The solvents were discarded and replaced by deionized water. Then, the precipitates and the deionized water were vortexed. After that, the centrifugation steps were repeated for 15 minutes every cycle until the solutions turned pH-neutral. Then, the samples were ready for freeze-drying. Following a similar procedure, the blank encapsulations were prepared without the addition of AI extracts. Next, the one parameter-at-a-time (OFAT) studies and optimization followed the same procedures. The process is illustrated in Figure 2.

Encapsulation Efficiency of Chitosan-PCL Determination

Firstly, a series of wavelength screenings were done under ultraviolet-visible (UV-VIS) spectrophotometers from 200–1000 nm on the crude AI extract samples. The highest peak was detected at 285nm and was used as a benchmark for the highest amounts of active compounds in the crude extracts of AI.

In another experiment, the encapsulated AI extracts were released from its Chitosan-PCL microcapsules by dissolving in 1.0 mL of 99.8% ethanol to determine the percentage of

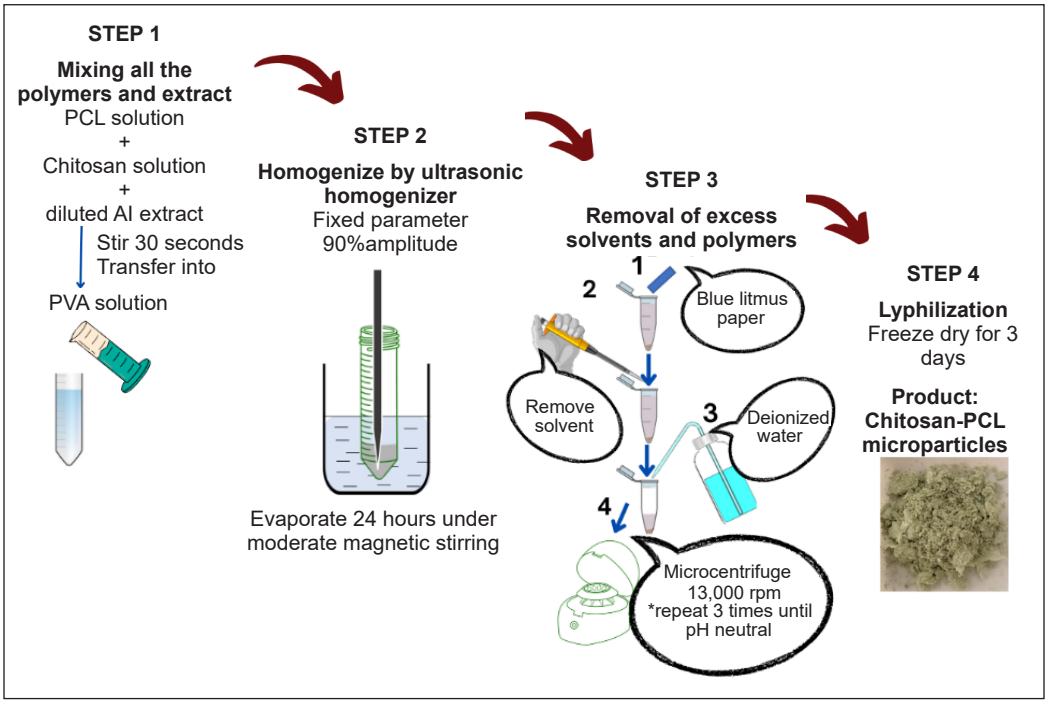

Figure 2. Schematic diagram of the emulsion-solvent evaporation method

encapsulation of AI extract entrapped in the microcapsule. The samples were centrifuged at 13,000 rpm for 1 hour. After that, the supernatant was collected and spectrophotometrically assayed at 285 nm. The amount of AI extracts entrapped was calculated using Equation 1.

$$EE\% = \frac{concentration \quad of \ extract \ \ in \ the \ microcapsules}{Initial \ \ concentration \quad of \ \ AI \ extracts} \times \ 100\% \qquad [1]$$

Optimization of Microencapsulation Process

The experiment was continued with a series of OFAT to find the preferred range for each parameter and select the desired range and levels for response surface methodology (RSM). In this experiment, only one parameter was manipulated, while the other parameters remained constant. Each run was repeated thrice.

Homogenization Duration. The OFAT of homogenization duration was conducted in four different durations, as shown in Table 1. Homogenization duration, which gave the highest encapsulation efficiency, was chosen for the next OFAT step based on the highest encapsulation efficiency (EE%) as the response.

Ratio of Chitosan:PCL Concentration. With the homogenization duration fixed at 5 minutes, the second OFAT of the Chitosan:PCL concentration ratio was conducted, where

the values were varied, as shown in Table 2. The ratio that gave the highest EE% was chosen for the next OFAT step.

PVA Concentration. With the ratio of Chitosan:PCL concentration fixed at 0.6:0.4, the third OFAT of PVA concentration ratio was conducted, where the values varied, as shown in Table 3—similarly, the highest EE% as the response was recorded and carried out for the next step.

Concentration of Chitosan-PCL Blends. With the PVA concentration fixed at 0.05%, the fourth OFAT of Chitosan-PCL blends concentration was conducted, where the values varied, as shown in Table 4, and EE% was recorded.

Table 1
Various homogenization durations of reaction using OFAT (Factor 1)

F1: Homogenization duration	F2: Chitosan:PCL concentration ratio (%)	F3: PVA concentration as a surfactant (%)	F4: Concentration of chitosan-PCL blends (%w/v)
3	0.5:0.5	2	1
5	0.5:0.5	2	1
7	0.5:0.5	2	1
10	0.5:0.5	2	1

Table 2
Various ratio concentrations of Chitosan:PCL using OFAT (Factor 2)

F1: Homogenization duration	F2: Chitosan:PCL concentration ratio (%)	F3: PVA concentration as a surfactant (%)	F4: Concentration of chitosan-PCL blends (%w/v)
5	0.2: 0.8	2	1
5	0.4: 0.6	2	1
5	0.5:0.5	2	1
5	0.6:0.4	2	1
5	0.8:0.2	2	1

Table 3
Various PVA concentrations using OFAT (Factor 3)

F1: Homogenization duration	F2: Chitosan:PCL concentration ratio (%)	F3: PVA concentration as a surfactant (%)	F4: Concentration of chitosan-PCL blends (%w/v)
5	0.6:0.4	0.01	1
5	0.6:0.4	0.05	1
5	0.6:0.4	0.1	1
5	0.6:0.4	0.3	1
5	0.6:0.4	0.5	1
5	0.6:0.4	1	1
5	0.6:0.4	2	1

Table 4
Various concentrations of Chitosan-PCL blends using OFAT (Factor 4)

F1: Homogenization duration	F2: Chitosan:PCL concentration ratio (%)	F3: PVA concentration as a surfactant (%)	F4: Concentration of chitosan-PCL blends (%w/v)
5	0.6:0.4	0.05	0.33
5	0.6:0.4	0.05	0.67
5	0.6:0.4	0.05	1.00
5	0.6:0.4	0.05	1.33
5	0.6:0.4	0.05	1.67

Study on Interaction Between Variables by Central Composite Design (CCD) for Surface Response Methodology (RSM)

The experiment was continued with the interaction study by response surface methodology (RSM). Central composite design (CCD) was chosen as the response surface model. The design of the experiment was aided by Design-Expert version 12 software using central composite design (CCD) to study the impact and interactions of independent variables.

Since the DOE software is unable to process the ratio values, the values used were only integer numbers. For instance, in the first factor, which is the ratio of chitosan to PCL, the value 4 means the ratio of chitosan to PCL was 0.4:0.6. Table 4 illustrates the values for the coded levels used in the DOE. For the fourth factor, the range of concentration of Chitosan-PCL blends (%w/v) in this study was limited according to the maximum concentration of chitosan that reached the gelation point for dissolution in 0.2% v/v of acetic acid. A preliminary experiment was done to find the maximum concentration reaching the gelation point. It was found that the chitosan reached the gelation point at a 1% g/mL concentration.

Thus, three factors were used to study the interactions. The independence variables of chitosan:PCL concentration ratios (X1), PVA concentration (X2), and the Concentration of chitosan-PCL blend (X3) were selected with the specific range obtained from the single experiments, OFAT. Details of the value of codified levels are tabulated in Table 5.

In CCD, three factors and one response were decided for the optimization study, and to predict the response at any point, codified units are the cube with the side [-1,1]. The design of CCD was proposed in Table 6 and simplified with the value of the coded units.

Table 5
Codified level for independent variables used in CCD for encapsulation optimization

Independent variables	Units	Coded levels		
		-1	0	+1
X1: Ratio of Chitosan (n) :PCL (10-n)	N chitosan	4	6	8
X2: PVA concentration	%	0.01	0.05	0.09
X3: Concentration of chitosan-PCL blend	%	0.6	1	1.4

Table 6
Design matrix of codified variables for central composite design

	Code			Experimental		
Run	Factor 1: Chitosan:PCL ratio	Factor 2: PVA concentration	Factor 3: Drug:polymer ratio	Factor 1: Chitosan:PCL ratio (%)	Factor 2: PVA concentration	Factor 3: Concentration of chitosan-PCL blend
1	-1	1	-1	4	0.09	0.6
2	1	1	-1	8	0.09	0.6
3	-1	1	1	4	0.09	1.4
4	1	-1	1	8	0.01	1.4
5	1	1	1	8	0.09	1.4
6	1	-1	-1	8	0.01	0.6
7	1	0	0	8	0.05	1
8	-1	-1	1	4	0.01	1.4
9	0	-1	0	6	0.01	1
10	0	1	0	6	0.09	1
11	-1	-1	-1	4	0.01	0.6
12	0	0	-1	6	0.05	0.6
13	0	0	0	6	0.05	1
14	0	0	1	6	0.05	1.4
15	0	0	0	6	0.05	1
16	0	0	0	6	0.05	1
17	-1	0	0	4	0.05	1

Model Validation

A validation study is an additional set of experiments carried out to validate and reproduce the output from the model. This study conducted two additional experiments referring to the new optimized parameters suggested by the DOE software. These two experiments were selected according to the highest and lowest EE% response predicted by DOE software. Subsequently, these two optimum samples were used for further characterizations.

Characterizations

Scanning Electron Microscope (SEM). A scanning electron microscope (SEM) (JEOL JSM-IT 100 InTouchScope™) accelerated at 5 kV was used to examine the morphological surface of the selected microparticles. The samples were coated with sputter coating (QC7620, Quorum Ltd, London) by placing the samples on the Nisshin EM conductive carbon tape that acted as a sample holder. The prepared samples were placed in a brass holder under the vacuum holder.

Fourier-Transform Infrared Spectroscopy (FTIR). The Fourier-transform infrared spectroscopy (FTIR) examination of the selected AI extract microencapsulation was determined using Nicolet iS50 FT-IR spectrophotometer (Thermo Scientific, Massachusetts, US). The samples in powder form were scanned under the regions of 4000–400 cm^{-1} wavenumber.

Particle Size Analysis and Zeta Potential. The average particle size was quantified using the dynamic light scattering (DLS) technique by Zetasizer Nano (Malvern Instruments Inc., UK). The system temperature was 25°C, the repetition was thrice, the Viscosity (cP) was 1.2, and the count rate (kcps) was 139.2. The refractive index of the material was 1.59. The microparticles were suspended in ethanol.

RESULTS AND DISCUSSIONS

Effects of OFAT Studies

Homogenization Duration. In Figure 3, encapsulation efficiency exhibited an upward trend from 3 minutes to 5 minutes of homogenization. During 3 minutes of duration homogenization, the oil/water phases did not completely break into smaller droplets. The physical observations were made from the solutions after solvent removal steps through 130 rpm/60 minutes centrifugations. Through observation in Figure 4, the solutions turned more translucent as the sonication time increased, and more precipitates were deposited. The microparticles recovered from centrifugation were similarly reported by Leong et al. (2017). From centrifugation, fewer microparticles were deposited, and the supernatant was slightly cloudy. During this time, the emulsification occurred incompletely.

After 5 minutes of homogenization, it is unlikely to result in any significant changes in encapsulation efficiency and the SEM images, but the trend of encapsulation efficiency declined. As the duration of homogenization increased, the input energy also increased, thus boosting the shear force due to acoustic cavitation. Due to this phenomenon, as time passes, more energy is dissipated to break down the larger oil/water molecules into smaller droplets (Abriata et al., 2019; Taha et al., 2020). According to Eric et al. (2017), this short homogenization duration may also result in the formation of coarse emulsion and a larger diameter of

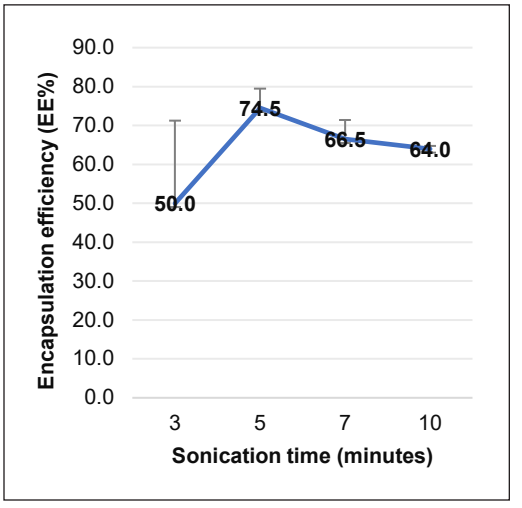

Figure 3. The effect of homogenization duration on the chitosan:PCL encapsulation efficiency

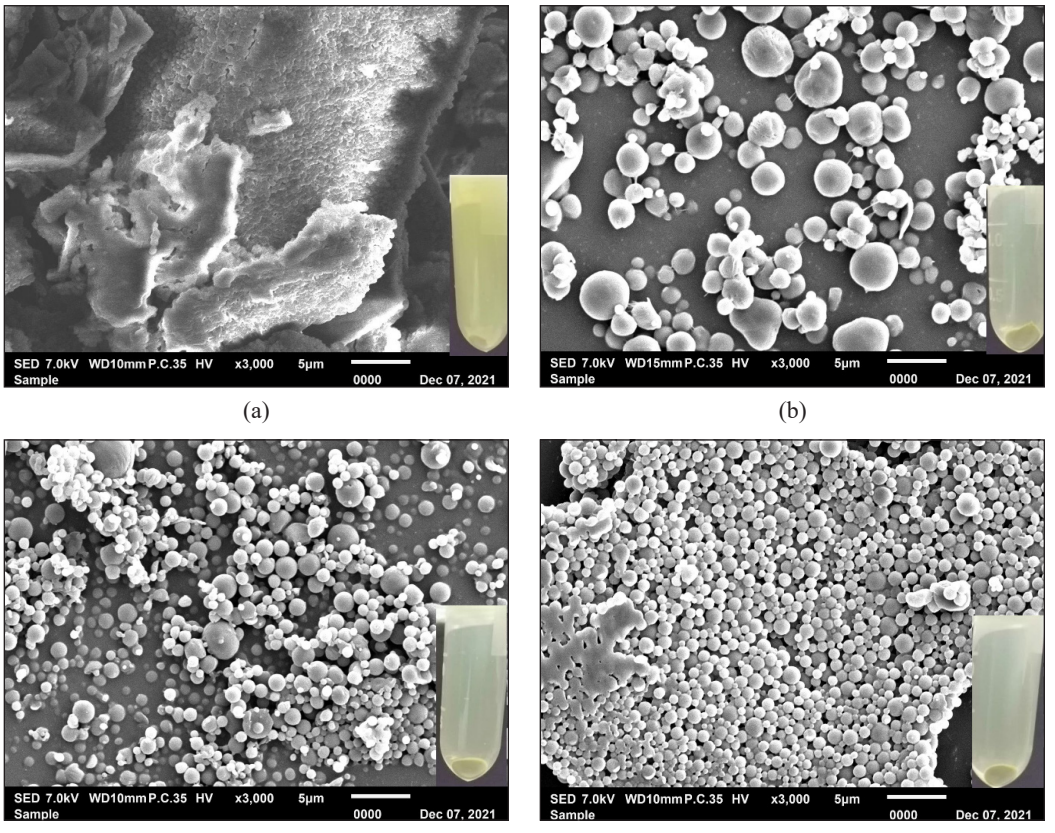

Figure 4. SEM images and visual register of the suspensions of samples at different homogenization durations: (a) 3 minutes, (b) 5 minutes, (c) 7 minutes, and (d) 10 minutes

emulsion droplets. Ten minutes duration somehow observed a good encapsulation image, but the EE% was lower than 5 and 7 minutes. The longer exposure time of the samples to homogenization may reduce the cavitation efficiency of the microtips and eroded (Taha et al., 2020). Through this experiment, 5 minutes of homogenization duration was selected and used in the next experiments.

The Ratio of Chitosan: PCL Concentration. The composition of chitosan and PCL is one of the most prioritized parameters that make up the concentration of chitosan-PCL blend as the carrier matrix. Figure 5 shows that the combination of a higher amount of PCL (0.2:0.8) resulted in the lowest EE% (33.80%). The EE% increased as the concentration of chitosan and PCL increased until the concentration of chitosan was more than PCL (0.6:0.4). Thus, the optimum concentration of chitosan and PCL obtained was 0.6 and 0.4 %w/v respectively with 70.10% EE%. The decrease of EE% after the 0.6 %w/v concentration of chitosan is possibly related to the viscosity of chitosan. In this case, the 0.8%w/v concentration of

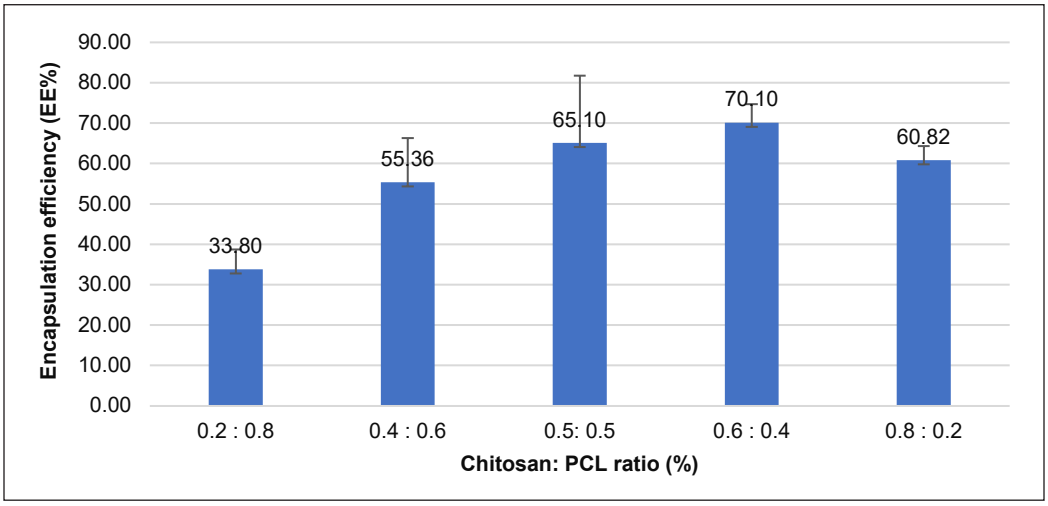

Figure 5. Chitosan-PCL copolymer encapsulation with AI extract with various ratios of chitosan:PCL

chitosan dissolved in 0.2%w/v acetic acid started to reach the gelation point. Thus, during the homogenization process, the chitosan molecules are unable to break well into smaller sizes, and the entrapment due to the chitosan not fully dissolved because the higher viscosity will reduce the intensity of the acoustic cavitation (Taurozzi et al., 2012).

Homopolymer (PCL only and Chitosan only) encapsulation does not form stable microencapsulation because, during opening or pore creation, the monomer droplets formed are very porous, unable to hold the extract, and the extract has been leaked out during the cavitation process before they start forming microemulsion (Taha et al., 2020). Unlike the heteropolymer encapsulation, while depolymerization occurs, both monomers of PCL and chitosan incorporate together, thus capping the AI extract inside. Less viscous liquid (e.g., water) undergoes cavitation more easily and becomes an emulsion phase (O/W). In summary, the ratio of 0.6:0.4 was selected for the next optimization.

The Surfactant (PVA) Concentration. A surface active agent commonly known as a surfactant used in this study is polyvinyl alcohol (PVA). PVA is a non-ionic surfactant, which is a nonelectrolyte. The emulsified droplets of chitosan-PCL-loaded AI extract microencapsulation need a surfactant to preserve stability as well as prevent continuous phase separation by coalescence (Leong et al., 2009).

As a stabilizer, the presence of PVA in the outer space of microparticles significantly affects the percentage of encapsulation efficiency. The maximum encapsulation efficiency was found when the concentration of PVA was 0.05%, which is 86.17% supported by the uniformly arranged morphological structure as in Figure 7. According to Figure 6, the trend of EE% started to decrease after 0.1% w/v from 74.17 to 71.11%. Thus, only 0.05% PVA is needed to reach the maximum encapsulation efficiency, 86.17%. The more PVA used, the

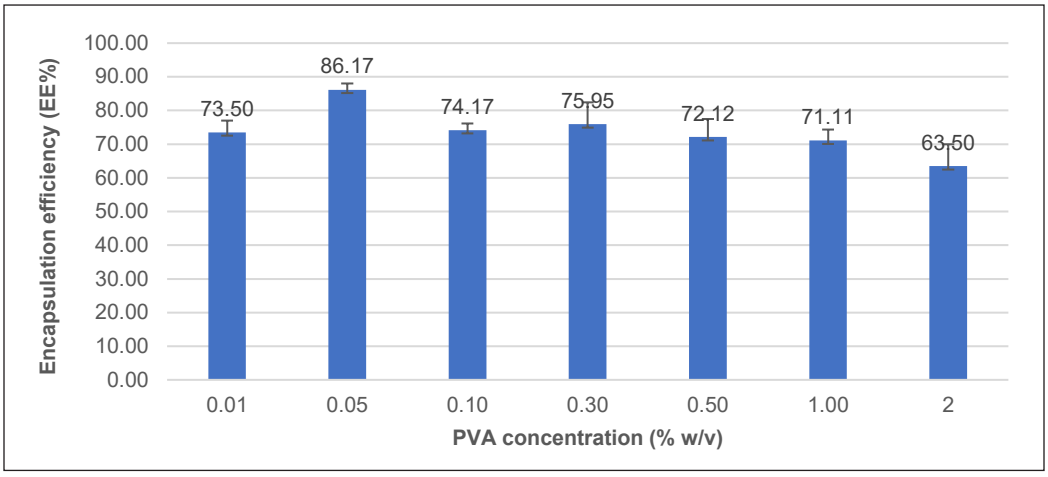

Figure 6. Effect of various PVA concentrations on encapsulation efficiency

higher the viscosity of the microemulsions, resulting in low encapsulation efficiency (Li et al., 2017).

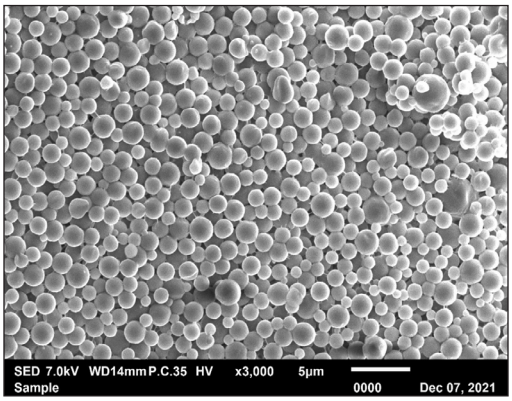

Figure 7. SEM image for 0.05% PVA

The Concentration of the Chitosan-PCL Blend

The concentration of the chitosan-PCL blend is an additional parameter that determines the amount of the carrier (chitosan-PCL blend) required for optimal encapsulations. The amount of AI extracts used was 0.2% concentration and kept constant for this study. The polymer matrix concentration study was limited according to the maximum concentration of chitosan that reaches the gelation point when dissolved in 0.2% v/v acetic acid glacial. Figure 8 shows that the maximum Chitosan-PCL blend concentration was obtained at a concentration of 1.0%, which resulted in 92.33% of EE—beyond 1% polymer concentration, which resulted in a decrease in EE. This trend of EE% was also observed by Iqbal et al. (2015) and El Hady et al. (2019). It was due to the viscosity of the polymer that caused the AI extract entrapment to become less efficient. The increase in polymer concentration also increased the thickness of the polymer matrix.

Response Surface Methodology

Table 7 shows ANOVA analysis for three factors, which are chitosan:PCL, PVA concentration, and polymer matrix concentration. The analysis shows that the model

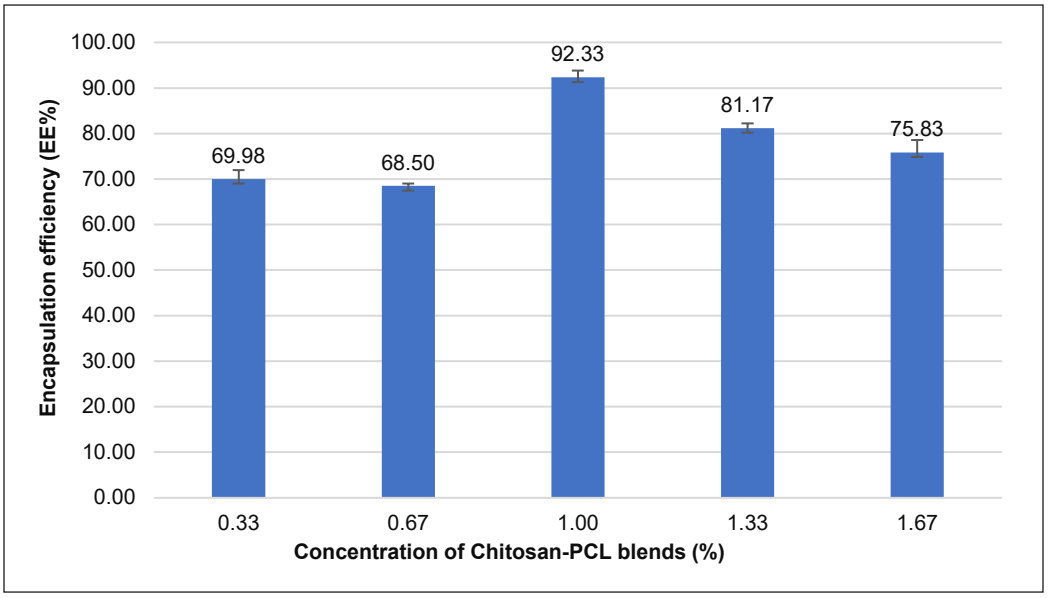

Figure 8. Concentration of Chitosan-PCL blends

Table 7
The analysis of variance for the encapsulation efficiency

Source	Sum of Squares	df	Mean Square	F-value	p-value	Remark
Model	5.562×10^{11}	8	6.952×10^{10}	14.25	0.0006	significant
A-Chitosan (n) :PCL (10-n) ratio	1.935×10^{11}	1	1.935×10^{11}	39.66	0.0002	
B-PVA concentration	8.209×10^{9}	1	8.209×10^{9}	1.68	0.2308	
C- Concentration of Chitosan-PCL blends	2.259×10^{11}	1	2.259×10^{11}	46.31	0.0001	
AC	2.973×10^{10}	1	2.973×10^{10}	6.09	0.0388	
BC	3.241×10^{9}	1	3.241×10^{9}	0.6643	0.4386	
A^2	3.100×10^{9}	1	3.100×10^{8}	0.0635	0.8074	
B^2	3.314×10^{10}	1	3.314×10^{10}	6.79	0.0313	
C^2	7.568×10^{9}	1	7.568×10^{9}	1.55	0.2482	
Residual	3.903×10^{10}	8	4.879×10^{9}			
Lack of Fit	2.72×10^{10}	6	4.536×10^{9}	0.7676	0.6611	not significant
Pure Error	1.182×10^{10}					
Cor Total	5.952×10^{11}					
R^2	0.9344					
Adjusted R^2	0.86890					
Predicted R^2	0.7105					
Adeq. Precision	13.0331					
Std. Dev	69848.92					
Mean	4.874×10^{5}					

F-value is 14.25, which implies that the model was significant, determined by a *p*-value <0.001. The regression coefficient (R^2) recorded was higher than 0.9, which is 0.9344, indicating that the experimental data was relatively strong. The difference between the adjusted coefficient of determination (R^2) and predicted R^2 was less than 0.2, considered reasonable agreement. The lack of fit was reported as not significant, meaning that the polynomial model fitted well and was statistically accurate (Li et al., 2017).

The 3D contour plot graphs predicted the interaction between the parameters, as shown in Figures 9 and 10. This study revealed difficulties finding the optimum conditions as the contour lines raised continuously and the shape became slightly sharp. It could be due to some limitations of the ultrasonic homogenization device contributing to external factors such as the condition of the microtips of ultrasonic homogenizer getting less efficient after many times usage. Another external factor is the temperature of the solutions during the encapsulation process. The heat dissipated during homogenization may lead to dichloromethane evaporation and decreased volume of the reacted solution (Taurozzi et al., 2012).

Figure 10 shows the linear interaction between the chitosan: PCL ratio and the polymer matrix concentration. As one increased the ratio of the chitosan:PCL, the EE% kept increasing, and while the polymer matrix concentration increased, the EE% decreased. As the concentration of the polymer matrix increased, the concentration of chitosan and PCL also increased while the ratio was maintained. This case happened due to the increasing concentration of chitosan, increasing the viscosity and hindering the ultrasonic homogenizer from breaking apart the chitosan molecules to form encapsulation (Taha et al., 2020). Figure 10 shows the relationship between PVA concentration and the concentration of the

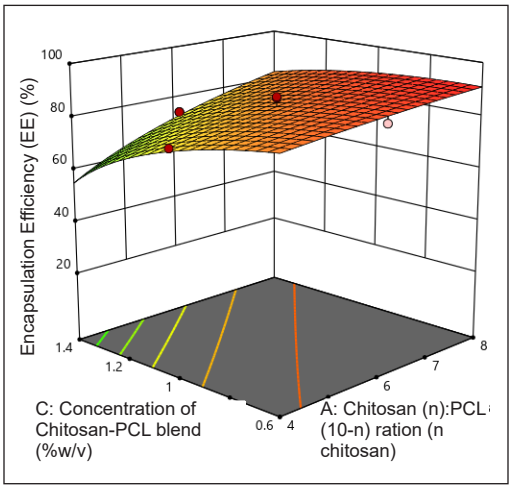

Figure 9. AC: The 3D model surface relationship between the ratio of chitosan:PCL and Polymer matrix concentration

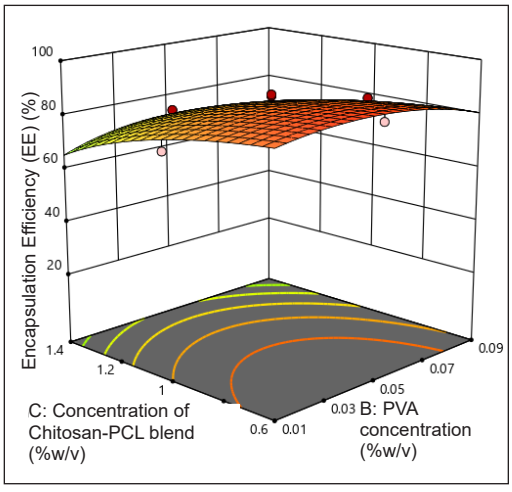

Figure 10. BC: 3D model surface relationship between PVA concentration and concentration of Chitosan-PCL blend

chitosan-PCL blend. The EE% started to increase and decrease as the polymer matrix and PVA concentration increased. In this case, only a small amount of PVA is needed to form a good encapsulation.

Next, based on this model, the second-order polynomial equation of the encapsulation efficiency was fitted into the coded Equation 2. The following equation obtained represents the quantitative effects of three factors on the encapsulation efficiency (EE%).

$$Y = 5.904 \times 10^5 + 1.391 \times 10^5 \times A - 28650.51 \times B - 1.503 \times 10^5 \times C + 60960.18 \times AC + 20128.31 \times BC - 10755.73 \times B^2 - 53148.54 \times C^2 \quad [2]$$

Model Validation

Validation has been done to determine the validity of the hypothesized model, and the details are tabulated in Table 8. The formulations with high and low EE% were chosen as used for the next analysis. It was found that the difference between the predicted value from DOE and the experimental value was not much different and reasonable. The experimental values revealed that the prediction of DOE was acceptable. The highest EE% recorded was beyond the expectation, which is 98.7%, as compared to the predicted 91.30%, and the error was 7.5%. However, the lowest EE% prediction value was recorded. The experimental value was within the predicted range, and the error was 1.2%, which is acceptable.

Table 8
Validation test of the model

	Factors			Encapsulation efficiency (EE %)		Error (%)
Run	Chitosan (n) :PCL (10-n) ratio	PVA concentration	Concentration of Chitosan-PCL blends	Predicted value from DOE	Experimental value	
1	8	0.042	0.648	91.30	98.70	7.5
39	5.216	0.052	0.6	86.75	87.80	1.2

Characterization

Structural Properties by FTIR. The spectra graph of the encapsulated Chitosan-PCL loaded AI extract, the encapsulated Chitosan-PCL blank, PVA, PCL, chitosan and AI extract were obtained and compared as in Figure 11.

The Chitosan parent chain is known to have an amino glucose structure linked with an amide linkage. Due to the presence of two strong functional groups, chitosan was capable of being modified to improve the limitations of chitosan. The two important functional groups are two hydroxyl groups and one primary amine group. Under the IR spectrum, the chitosan in powder form was tested, and a broad peak between 2940–2860 cm^{-1} was exposed. The chitosan spectra can be detected due to the existence of amide I and amide II. Amide I was detected at 1650 cm^{-1} associated with C=O stretching vibration. Amide II

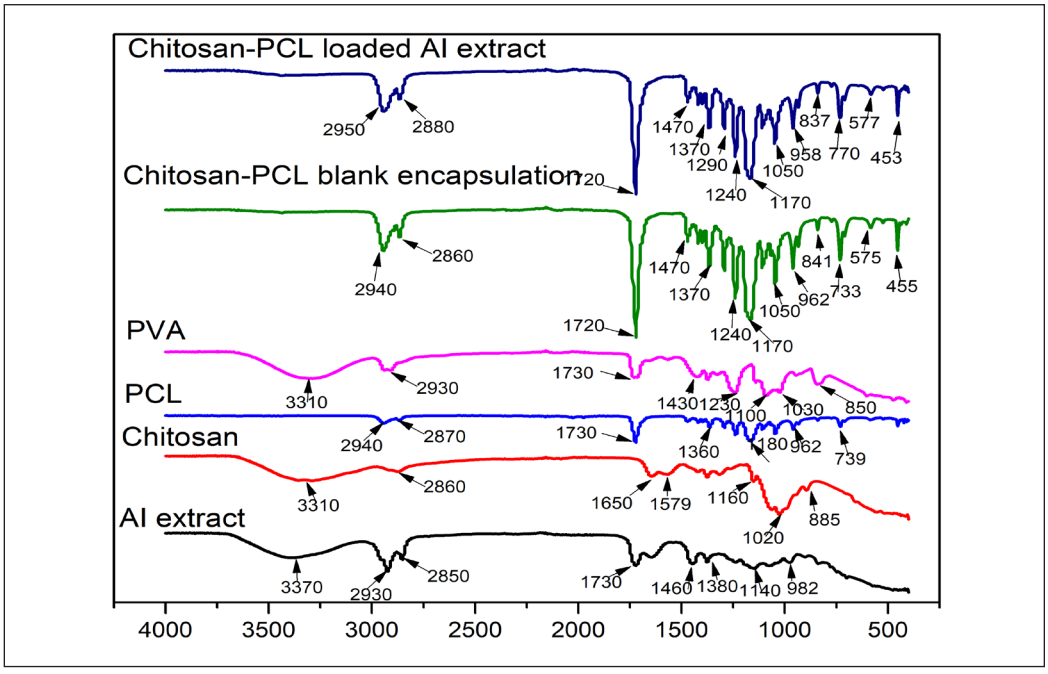

Figure 11. FTIR spectra for AI extract, chitosan, PCL, PVA, chitosan-PCL blank encapsulation and chitosan-PCL loaded AI extracts

was detected at 1579 cm-^{1}, which is associated with and recognizable by N-H stretching. The C-H stretching was detected at 2860 cm^{-1}. The ß-linked glycosidic bond was detected at 885 cm^{-1}. 1020 cm^{-1} indicated the absorbance of O bridge stretching of glucosamine residue present. The characteristics of PCL were detected from the peak at 2940 cm^{-1}, which is the asymmetric vibration stretching for the -CH_3 group, and 2870 cm^{-1}, which is the -CH_2 (methylene) stretching. The stretching on 1730 cm^{-1} indicated the C=O (ketone). The band stretching at 1360 cm^{-1} indicated the presence of the C-O-C group, followed by more vibration bands by asymmetric stretching at 1180, 962, and 739 cm^{-1}.

The interaction of the polymer compositions showed characteristic bands at 2950-2880 cm^{-1} (C-H stretching); the spectra in PCL were switched from 1730 to 1720 cm^{-1}, which indicated ketone and several inorganic ions from 1370–453 cm^{-1}, in which the similar bands existed in the single ingredients. Ultimately, similar findings were reported by Almeida et al. (2018). The encapsulation of AI extracts was successful through the presence of characteristic bands of chitosan, PCL, and the AI extracts. On the IR spectrum of chitosan-PCL loaded AI extracts, the presence of a sharp peak at 1470cm^{-1} indicates the characteristic of Amide II of chitosan. The presence of PCL was detected through the strong characteristic band of ketone at 1720 cm^{-1}. The characteristic band of AI extracts were expressed at 1470 and 1370 cm$^{-1,}$ showing the interactions of AI extracts occurred. Based on the FTIR spectra, the encapsulation of AI extract with chitosan-PCL blend occurred and can be suggested.

Surface Morphology by Scanning Electron Microscope (SEM). The SEM images exhibited the formation of spherical shapes with smooth surfaces for the sample with the highest EE% (98.70%) in Figure 12(a) and less polydisperse. In Figure 12(b), the surface morphology of the encapsulation with lower EE% (87.80%) also showed a spherical shape.

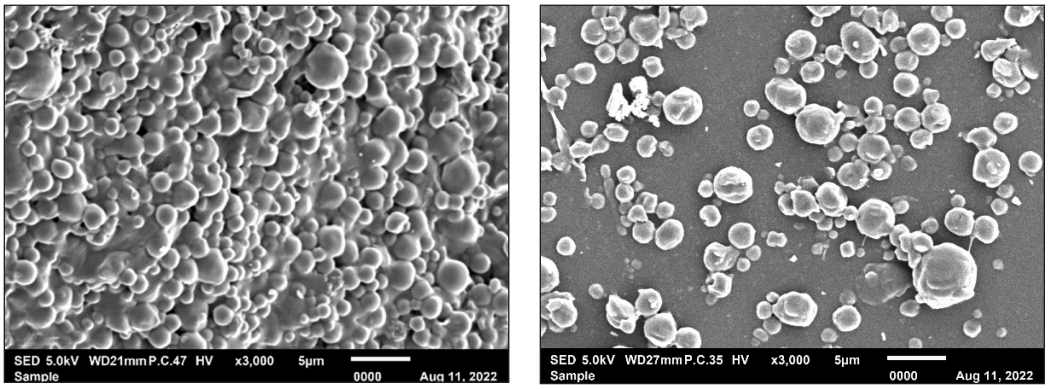

(a) (b)

Figure 12. SEM image for chitosan-PCL loaded AI extract with (a) EE 98.70% and (b) 87.80%

Zeta Potential and Particle Size Analysis. Table 9 summarizes the findings on the effects of zeta potential and particle size on the EE% of the AI extract microencapsulations. In this study, the values of zeta potential were negative due to the adsorption of the surfactant on the surface of the microparticles (Abriata et al., 2019). Interestingly, most encapsulations of plant extracts studies reported found in agreement with the negative value of zeta potential obtained from this study. In 2020, the encapsulation of *Boswellia carterii* essential oil by Barre et al. (2020) found that the zeta potential was -25 to -36 mV. In 2021, the encapsulation of phenolic bioactive compounds found the zeta potential was -30 to -44 mV (Xue et al., 2021).

This result was an improvement from the previous AI extracts encapsulation study reported by Amarnath et al. (2014) and Muhaimin et al. (2020), in which the zeta potential obtained was -3.47 mV.

The high EE% was obtained from the small size of particles. The small particle size may entrap more active ingredients of AI extract, thus giving a higher EE%. The smaller

Table 9
The zeta potential and particle size for the optimized samples

Sample validation number	Encapsulation efficiency (EE%)	Zeta potential (mV)	Particle size (μm)
1	98.70	-24.0	2.631 ± 0.14
39	87.80	-26.2	3.568 ± 1.35

size also led to the microparticles being absorbed and the active ingredients being released to the targeted parts. The particle size obtained was similar to that obtained by Amarnath et al. (2014), which encapsulated the AI extract with chitosan-casein, which was 2µm. Another encapsulation study of *M. gigantea* leave extracts obtained 3.6–5.9 µm in size (Muhaimin et al., 2020).

CONCLUSION

In conclusion, 5 minutes of the best homogenization duration has resulted in the highest encapsulation efficiency (74.5%). The other three parameters, the 0.6:0.4 ratio of Chitosan:PCL concentration was 70.10%, 0.05% concentration of PVA giving 86.17%, and the 1% concentration of Chitosan-PCL blend was 92.33% have successfully found the optimized value. The values for the parameter interaction studies were obtained by applying the central composite design (CCD) using Design-Expert v.12 software. In the validation process, the highest EE% obtained was 98.70%, and the lowest EE% was 87.80%. Surface morphology showed the spherical shape of microparticles. The zeta potential for both higher EE% and lower EE% microencapsulations resulted in a small difference. Overall, the encapsulation of *Acalypha indica* (AI) extracts has been successfully done using chitosan-PCL copolymer blends by emulsion-solvent evaporation. This research has a high potential to explore the usage of AI in pharmaceutical applications.

ACKNOWLEDGEMENTS

This work was financially supported by a Collaborative Research grant (CRG) from Universiti Teknologi Malaysia (UTM) (Q.J130000.2451.08g10) and the University of Technology Malaysia (UTM) Fundamental Research Grant (Q.J130000.3846.22H56). The author thanks Kulliyyah of Engineering, International Islamic University Malaysia (IIUM), for providing the laboratory facilities.

REFERENCES

Abriata, J. P., Turatti, R. C., Luiz, M. T., Raspantini, G. L., Tofani, L. B., do Amaral, R. L. F., Swiech, K., Marcato, P. D., & Marchetti, J. M. (2019). Development, characterization and biological *in vitro* assays of paclitaxel-loaded PCL polymeric nanoparticles. *Materials Science and Engineering C, 96*, 347-355. https://doi.org/10.1016/j.msec.2018.11.035

Adepu, S., & Ramakrishna, S. (2021). Controlled drug delivery systems: Current status and future directions. *Molecules, 26*(19), Article 5905. https://doi.org/10.3390/molecules26195905

Amarnath, K., Dhanabal, J., Agarwal, I., & Seshadry, S. (2014). Cytotoxicity induction by ethanolic extract of *Acalypha indica* loaded casein-chitosan microparticles in human prostate cancer cell line *in vitro*. *Biomedicine and Preventive Nutrition, 4*(3), 445-450. https://doi.org/10.1016/j.bionut.2013.03.009

Barre, M. S., Ali, F. B., Mirghani, M. E. S., Hazri, N. F., Anuar, H., & Nasir, N. A. M. (2020). Potential food additive of *Boswellia carterii* essential oil encapsulated within gum arabic: A particle size distribution and zeta potential analysis. *Food Research, 4*, 19-23. https://doi.org/10.26656/fr.2017.4(S2).339

Bazana, M. T., Codevilla, C. F., & de Menezes, C. R. (2019). Nanoencapsulation of bioactive compounds: Challenges and perspectives. *Current Opinion in Food Science, 26*, 47-56. https://doi.org/10.1016/j.cofs.2019.03.005

Christen, M. O., & Vercesi, F. (2020). Polycaprolactone: How a well-known and futuristic polymer has become an innovative collagen-stimulator in esthetics. *Clinical, Cosmetic and Investigational Dermatology, 13*, 31-48. https://doi.org/10.2147/CCID.S229054

El Hady, W. E. A., Mohamed, E. A., El-Aazeem S. O. A., & El-Sabbagh, H. M. (2019). *In vitro-in vivo* evaluation of chitosan-PLGA nanoparticles for potentiated gastric retention and anti-ulcer activity of diosmin. *International Journal of Nanomedicine, 14*, 7191-7213. https://doi.org/10.2147/IJN.S213836

Iqbal, M., Valour, J. P., Fessi, H., & Elaissari, A. (2015). Preparation of biodegradable PCL particles via double emulsion evaporation method using ultrasound technique. *Colloid and Polymer Science, 293*(3), 861-873. https://doi.org/10.1007/s00396-014-3464-9

Leong, T. S. H., Martin, G. J. O., & Ashokkumar, M. (2017). Ultrasonic encapsulation - A review. *Ultrasonics Sonochemistry, 35*, 605-614. https://doi.org/10.1016/j.ultsonch.2016.03.017

Leong, T. S. H., Wooster, T. J., Kentish, S. E., & Ashokkumar, M. (2009). Minimising oil droplet size using ultrasonic emulsification. *Ultrasonics Sonochemistry, 16*(6), 721-727. https://doi.org/10.1016/J.ULTSONCH.2009.02.008

Li, X., Wang, L., & Wang, B. (2017). Optimization of encapsulation efficiency and average particle size of *Hohenbuehelia serotina* polysaccharides nanoemulsions using response surface methodology. *Food Chemistry, 229*, 479-486. https://doi.org/10.1016/j.foodchem.2017.02.051

Muhaimin, M., Yusnaidar, Y., Syahri, W., Latief, M., & Chaerunisaa, A. Y. (2020). Microencapsulation of *Macaranga gigantea* leaf extracts: Production and characterization. *Pharmacognosy Journal, 12*(4), 716-724. https://doi.org/10.5530/pj.2020.12.104

Rivas, J. C., Cabral, L. M. C., & Rocha-Leão, M. H. (2019). Stability of bioactive compounds of microencapsulated mango and passion fruit mixed pulp. *International Journal of Fruit Science, 20*(S2), S94-S110. https://doi.org/10.1080/15538362.2019.1707746

Roy, S. M., & Sahoo, S. K. (2016). Controlled drug delivery: Polymeric Biomaterials for. *Encyclopedia of Biomedical Polymers and Polymeric Biomaterials, 11*, 2135-2146. https://doi.org/10.1081/e-ebpp-120050023

Szymańska, E., & Winnicka, K. (2015). Stability of chitosan - A challenge for pharmaceutical and biomedical applications. *Marine Drugs, 13*(4), 1819-1846. https://doi.org/10.3390/md13041819

Taha, A., Ahmed, E., Ismaiel, A., Ashokkumar, M., Xu, X., Pan, S., & Hu, H. (2020). Ultrasonic emulsification: An overview on the preparation of different emulsifiers-stabilized emulsions. *Trends in Food Science and Technology, 105*, 363-377. https://doi.org/10.1016/j.tifs.2020.09.024

Taurozzi, J. S., Hackley, V. A., & Wiesner, M. R. (2012). *Preparation of Nanoparticle Dispersions from Powdered Material using Ultrasonic Disruption*. U.S. Department of Commerce. http://dx.doi.org/10.6028/NIST.SP.1200-2

Xue, J., Luo, Y., Balasubramanian, B., Upadhyay, A., Li, Z., & Luo, Y. (2021). Development of novel biopolymer-based dendritic nanocomplexes for encapsulation of phenolic bioactive compounds: A proof-of-concept study. *Food Hydrocolloids, 120*, Article 106987. https://doi.org/10.1016/j.foodhyd.2021.106987

Yusuf, A., Almotairy, A. R. Z., Henidi, H., Alshehri, O. Y., & Aldughaim, M. S. (2023). Nanoparticles as drug delivery systems: A review of the implication of nanoparticles' physicochemical properties on responses in biological systems. *Polymers, 15*(7), Article 1596. https://doi.org/10.3390/polym15071596